ACS APPLIED MATERIALS & INTERFACES

Research Article

www.acsami.org

Light-Directed Self-Assembly of Robust Alginate Gels at Precise Locations in Microfluidic Channels

Hyuntaek Oh,[†] Annie Xi Lu,[†] Vishal Javvaji,[†] Don L. DeVoe,[‡] and Srinivasa R. Raghavan*[,†]

[†]Department of Chemical and Biomolecular Engineering and [‡]Department of Mechanical Engineering, University of Maryland, College Park, Maryland 20742, United States

Supporting Information

ABSTRACT: Recently there has been much interest in using light to activate self-assembly of molecules in a fluid, leading to gelation. The advantage of light over other stimuli lies in its spatial selectivity, i.e., its ability to be directed at a precise location, which could be particularly useful in microfluidic applications. However, existing light-responsive fluids are not suitable for these purposes since they do not convert into sufficiently strong gels that can withstand shear. Here, we address this deficiency by developing a new light-responsive system based on the well-known polysaccharide, alginate. The fluid is composed entirely of commercially available components: alginate, a photoacid generator (PAG), and a chelated complex of divalent strontium (Sr^{2+}) cations. Upon exposure to ultraviolet (UV) light, the PAG dissociates to release H^+ ions, which in turn induce the release of free Sr^{2+} from the chelate. The Sr^{2+} ions self-assemble with the alginate chains to give a stiff gel with an elastic modulus ~2000 Pa and a yield stress ~400 Pa (this gel is strong enough to be picked up and held by one's fingers). The above fluid is sent through a network of microchannels and a short segment of a specific channel is exposed to UV light. At that point, the fluid is locally transformed into a strong gel in a few minutes, and the resulting gel blocks the flow through that channel while other channels remain open. When the UV light is removed, the gel is gradually diluted by the flow and the channel reopens. We have thus demonstrated a remote-controlled fluidic valve that can be closed by shining light and reopened when the light is removed. In addition, we also show that light-induced gelation of our alginate fluid can be used to deposit biocompatible payloads at specific addresses within a microchannel.

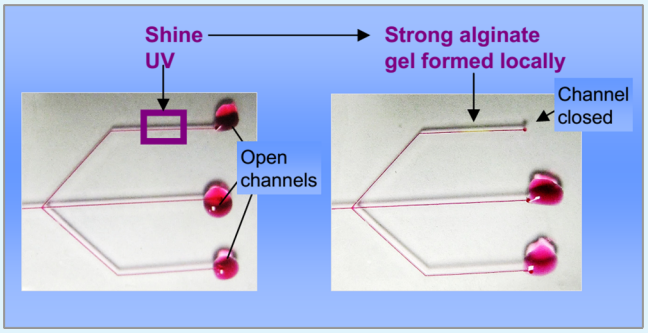

KEYWORDS: *photorheological fluid, photoresponsive self-assembly, microfluidic valve, photodeposition, ionic cross-linking*

INTRODUCTION

Fluids whose rheological properties can be remotely controlled by external fields have fascinated scientists and engineers. The first examples of such fluids date back to the 1940s and focused on rheology modulation via electric or magnetic fields, with the corresponding fluids being termed electrorheological (ER) and magnetorheological (MR) fluids, respectively.[1−4] Since that time, a wide range of applications have been envisioned for ER and MR fluids in mechanical devices such as dampers, clutches, and valves, some of which have been practically realized.[4,5] Recently, light has emerged as a different remote trigger for rheology modulation. Fluids with light-tunable rheology are termed photorheological (PR) fluids.[6] Light as an external trigger has many advantages over other fields or stimuli: it can be directed from a distance at a precise location with a resolution of few microns, and a wide range of light sources are available with distinct wavelengths and intensities. A potential application of PR fluids that would leverage the spatial selectivity of light is in making a light-activated valve for flow control within microfluidic or nanofluidic devices.[7] The idea is that, by using light as an external switch, specific flow paths within a network of fluidic channels can be closed and reopened as needed.

Despite many recent advances, PR fluids are not used in applications such as the one described above. There are many reasons for this. One major bottleneck that used to exist with PR fluid formulations is that they used to be based on complex photoresponsive molecules that needed to be synthesized for the purpose. Examples of such molecules include surfactants,[8−12] salts,[13−15] polymers,[16−18] or small-molecule gelators[19−21] that contain photoresponsive azobenzene, stilbene, or spiropyran moieties. In the past few years, however, our lab[22−29] and others[30−32] have developed PR fluids based entirely on simple, commercially available components (no synthesis required). For example, we recently demonstrated a surfactant-based PR fluid that shows a million-fold increase in its zero-shear viscosity under ultraviolet (UV) light and a decrease back to its original viscosity under visible light.[29]

Received: March 30, 2016
Accepted: June 9, 2016
Published: June 27, 2016

DOI: 10.1021/acsami.6b03826
ACS Appl. Mater. Interfaces 2016, 8, 17529−17538

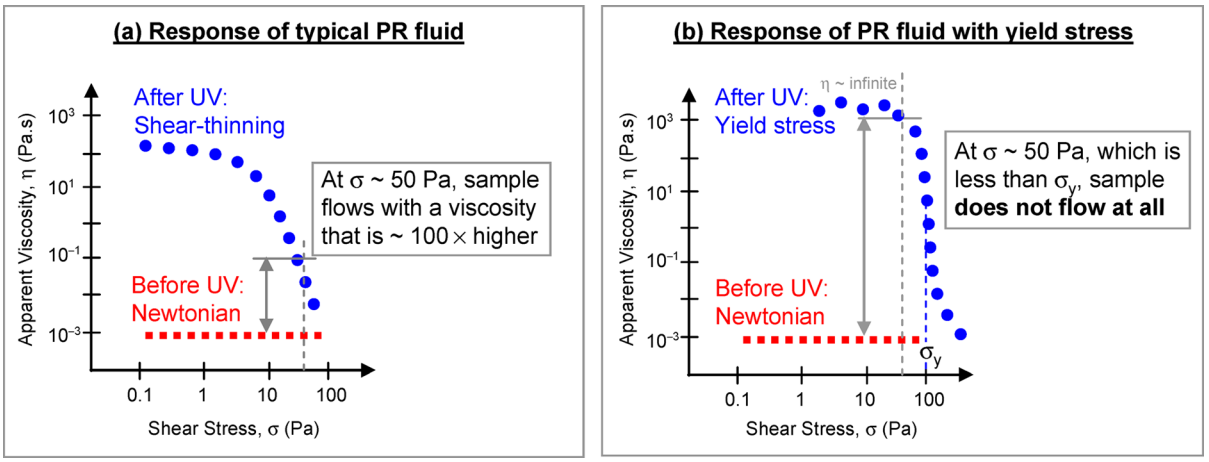

Figure 1. Comparing the rheology of two types of PR fluids. In both cases, initially, i.e., before UV irradiation, the sample is a low-viscosity Newtonian fluid. (a) Upon exposure to UV light, the sample attains a high, but finite low-shear viscosity followed by a decrease in viscosity under higher shear (shear-thinning). Thus, the ratio of viscosities at a stress σ = 50 Pa is only ~100×. (b) Upon exposure to UV light, the sample becomes a gel with a yield stress σ_y ~ 100 Pa, i.e., the viscosity is practically infinite for $\sigma < \sigma_y$. As a result, at σ = 50 Pa, the sample does not flow at all. The response in (b) is desirable for flow-blocking applications.

These simpler systems have made PR fluids accessible to many more researchers, which is expected to facilitate applications.

While the accessibility problem has been potentially solved, other issues remain. One issue for applications in microscale devices is that fluids in these devices can be subjected to very high shear rates (due to the small dimensions of the channels).[33,34] At these high shear rates, the PR effect is reduced, i.e., the light-induced change in viscosity tends to be insufficient to affect the flow. The problem arises because the high-viscosity state of all PR fluids relies on physical (noncovalent) bonds, i.e., on self-assembly.[11,19] These physical bonds tend to get disrupted when the fluid is sheared and re-form when shear is ceased. For this reason, PR fluids tend to show significant shear-thinning, i.e., a sharp decrease in their viscosity as a function of shear rate or shear-stress (Figure 1a).[35,36] Consequently, the light-induced change in viscosity at high shear may be small (only a factor of ~10 to 100) even though this change is substantial (factor of 1000 or more) at low shear, as shown in Figure 1a.

A further issue has to do with the time scale of light-induced rheological changes, i.e., the response time. Most PR fluids require relatively long irradiation times (more than 10 min) to induce a large change in viscosity, even when a high-power UV lamp (>100 W) is used. The response time is shorter for smaller sample volumes, i.e., it seems to depend mainly on the path length traversed by the light.[22,26] Thus, the response times for samples in microchannels (nL volumes) is expected to be much less than that for macroscopic samples in vials (mL volumes). However, if the fluid in the microchannel is flowing while being irradiated at a specific point, the response time becomes even more critical. That is, the sample rheology must be transformed quickly before fresh sample is brought to the irradiation point by the flow. Also, the pressure exerted by the flow will counteract the buildup of a viscoelastic plug. Thus, in order to block the flow and withstand the pressure buildup, there must be a rapid and substantial change in the fluid rheology.

In this paper, we develop a new PR fluid that can be used in a light-activated fluidic valve. Our new formulation addresses the issues detailed above. The fluid is converted by UV light from a thin liquid (sol) into a strong gel, and this conversion occurs relatively quickly. When this fluid flows through a network of microchannels, we can block the flow through a specific channel by irradiating a point in that channel with UV light for ~3 min. We show that the key to blocking the flow is the elastic character of the gel, as measured by its elastic modulus G' and its yield stress σ_y. Note that the viscosity of a gel, i.e., a material with a yield stress, is essentially infinite below the yield stress.[34,35] That is, a gel has an infinite relaxation time and viscosity, whereas these are both finite in the case of a viscoelastic fluid.[34,35] The importance of the yield stress is indicated by Figure 1b, i.e., for a fluid to block the flow, it should have a sufficient yield stress. Indeed, this point is well-known to scientists working on ER and MR fluids, who thus seek to maximize the yield stress under an electric or magnetic field.[4,37] Likewise, PR fluids need to exhibit substantial σ_y values in their gel state to be usable in flow-blocking applications (i.e., valves, clutches, and dampers).

How does one create a PR fluid that is based on simple components and yet gives a strong gel with a high yield stress? We ruled out micellar PR fluids because these generally form viscoelastic fluids and not gels.[11,29] Small-molecule gelators with PR properties can exhibit yield stresses,[19−21] but most of these systems require synthesis[38−40] and the yield stresses are not that high either. This leaves us with two candidates: PR fluids based either on nanoparticles[24] or on polymers.[26] Both these have been developed in our lab and both form gels with yield stresses when irradiated with UV light, but the σ_y values are not that high (~10 Pa). To provide a practical analogy, these were paste-like gels akin to ketchup; they were not free-standing solids, i.e., they could not be removed from their container and gripped by tweezers or one's fingers.

In order to increase the yield stress, we turn to a polymeric system based on sodium alginate. Alginate is a naturally occurring polysaccharide that is extensively used for cell encapsulation and other biomedical studies.[41,42] Typically, alginate solutions are cross-linked into gels by adding divalent cations like calcium (Ca^{2+}) or strontium (Sr^{2+}). Recently, several researchers have devised strategies to induce gelation of alginate by light.[43−48] This has been done either by attaching photo-cross-linkable groups to the alginate backbone[43,44] or by photoinduced release of divalent ions.[45,46] Here, to make

DOI: 10.1021/acsami.6b03826
ACS Appl. Mater. Interfaces 2016, 8, 17529−17538

alginate solutions light-responsive, we use a class of molecules called photoacid generators (PAGs).[49,50] The idea of using PAGs to create light-responsive self-assemblies was first reported by our lab[24,26] and since then has been used by several researchers in a variety of systems.[51−53] In our current system, we combine alginate, a PAG, and a chelated complex of Sr^{2+} ions to form a PR fluid. All these components are commercially available. The concept is shown in Figure 2 and is discussed further below. The net result upon shining UV light is to form an alginate gel cross-linked by Sr^{2+} ions, which is shown to exhibit σ_y > 100 Pa. This gel is strong enough to be lifted off the benchtop and held by one's fingers (Figure 2c). Because our system offers simplicity (using only common chemicals), a dramatic PR effect (from thin sol to strong gel), and a fast response (within a few minutes), we believe it will have wide utility. In addition to the fluidic valve, we also show a different application with this system involving the use of light to deposit payloads at specific addresses along the walls of microchannels.

EXPERIMENTAL SECTION

Materials. Sodium alginate from brown algae (product number 4-00005) was purchased from Carbomer. The molecular weight was specified by the manufacturer to be around 500 kDa. Alginate extracted from algae usually contains impurities, and therefore its solution is slightly turbid. To purify the alginate, it was dissolved in water at 1 wt % and the solution pH was adjusted to around 10 with NaOH. Suspended impurities in the solution were removed by filtration with Fisherbrand Glass Fiber Circles, grade G6, followed by precipitation with acetone. The final purified alginate gave a clear solution that was free of suspended impurities. The photoacid generator (PAG), diphenyliodonium nitrate, and methyl-β-cyclodextrin (m-β-CD) were purchased from TCI. The chelating agent, ethylene glycol tetraacetic acid, tetrasodium salt (EGTA), strontium chloride ($SrCl_2$), D-glucono-δ-lactone (GdL), and phenol red were obtained from Sigma-Aldrich. Aqueous solutions of green fluorescent beads (Fluoresbrite YG, 0.10 μm) and red fluorescent beads (Fluoresbrite Polychromatic Red, 0.5 μm) were purchased from Polysciences. For all samples, deionized (DI) water was used.

Sample Preparation. All samples were prepared by mixing stock solutions of alginate, Sr-EGTA, and the PAG-CD complex. The purified alginate was dissolved at a concentration of 5 wt % in DI water to make its stock solution. The Sr-EGTA solution was prepared by dissolving desired amounts of $SrCl_2$ and EGTA at a EGTA:$SrCl_2$ molar ratio of 1.25. To prepare the solution of the PAG-CD complex, weighed amounts of PAG and m-β-CD were dissolved in DI water, and this solution was sonicated for 5 min. The molar ratio of m-β-CD:PAG was fixed at 3. To make the PR fluids, equal volumes of the Sr-EGTA and the PAG-CD stock solutions were first mixed, and to this an equal volume of the alginate stock solution was added, followed by vortex mixing. The final concentration of alginate in the PR fluids was 2.5 wt %. The pH of these fluids before light irradiation was around 8.0.

Sample Response Before and After UV Irradiation. Samples were irradiated with UV light from an Oriel 200 W mercury arc lamp. A dichroic beam turner with a mirror reflectance range of 280 to 400 nm was used to access the UV range of the emitted light. A filter for below 400 nm light was used to eliminate the undesired visible wavelengths. Samples (2.5 mL) were placed in a Petri dish of 60 mm diameter with a quartz cover, and irradiation was done for a specific duration without stirring.

Rheological Studies. A TA Instruments AR2000 stress-controlled rheometer was used to perform steady and dynamic rheological experiments. Samples were run at 25 °C on a cone-and-plate geometry (40 mm diameter and 2° cone angle) or a parallel plate geometry (20 mm diameter). A solvent trap was used to minimize drying of the sample during measurements. Dynamic frequency spectra were conducted in the linear viscoelastic regime of the samples, as determined by prior dynamic strain sweeps.

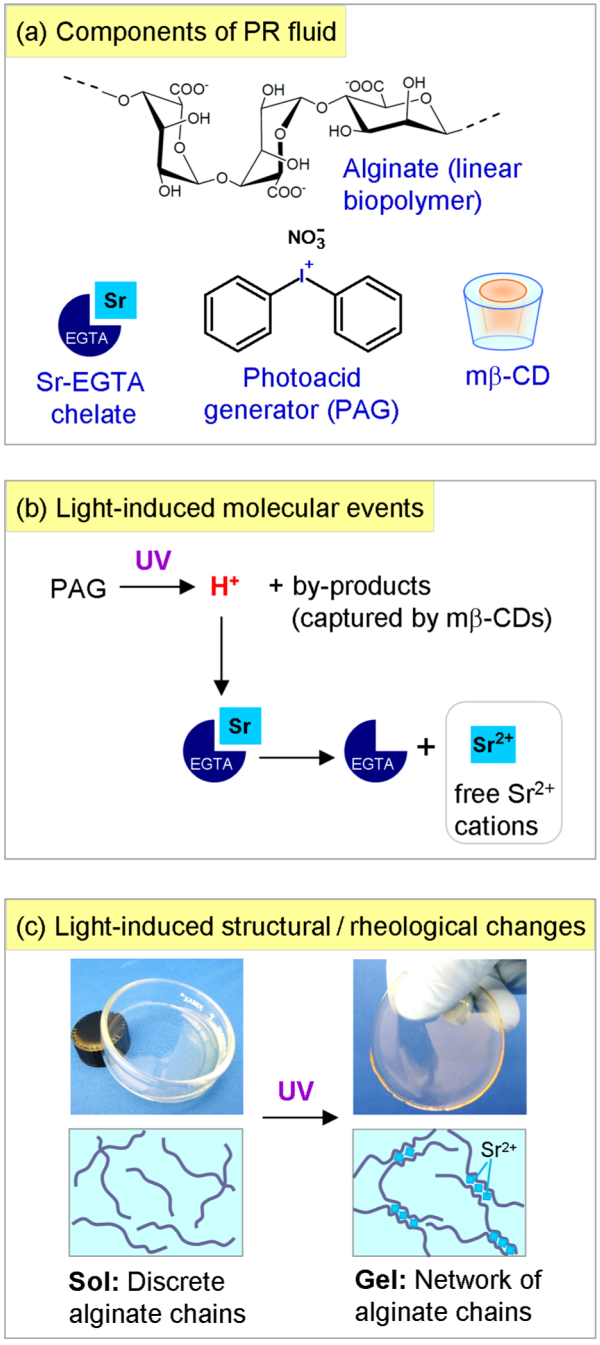

Figure 2. Working principle of the PR fluid developed in this study. (a) The components are the biopolymer alginate, the Sr-EGTA chelate, a photoacid generator (PAG), viz., diphenyliodonium nitrate, and a type of cyclodextrin (mβ-CD). When exposed to UV light, the following events occur at the molecular scale: (b) the PAG gets photolyzed, releasing acid (H^+), which induces the Sr-EGTA to dissociate and release free Sr^{2+}. Byproducts of PAG photolysis are sequestered within the binding pockets of mβ-CDs. The effects on the structure and rheology are shown in (c): free Sr^{2+} ions cross-link the alginate chains to form a strong gel that is rigid enough to be lifted by one's fingers, as shown by the photo.

Microfluidic Chip Fabrication and Operation. A plastic chip made from poly(methyl methacrylate) (PMMA) was used in this study. PMMA sheets (FF grade; 4 in. × 4 in. × 1/16 in.) were purchased from Piedmont Plastics and cut into two pieces to form the

DOI: 10.1021/acsami.6b03826
ACS Appl. Mater. Interfaces 2016, 8, 17529−17538

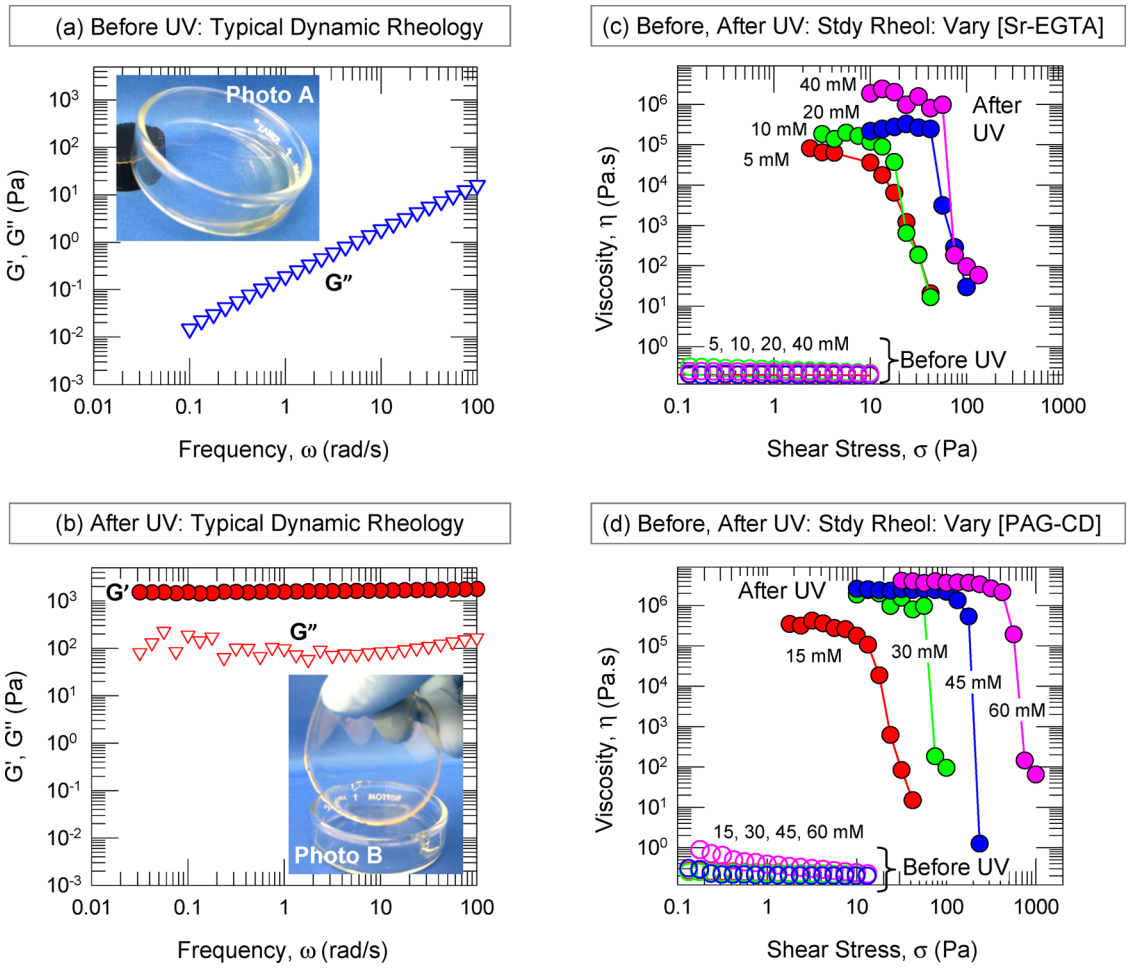

Figure 3. Rheology of PR fluids before and after exposure to UV light. Data from dynamic rheology for the elastic modulus G' and the viscous modulus G'' as functions of frequency ω are shown in (a) and (b) for a sample of 2.5 wt % alginate, 40 mM Sr-EGTA, and 30 mM PAG-CD. Before UV, the sample is a thin, viscous liquid (Photo A). After UV, the sample is a strong gel that can be lifted by one's fingers (Photo B). In (c) and (d), data from steady-shear rheology for the viscosity as a function of shear-stress are shown. Data before UV are represented as unfilled circles while that after UV is shown by filled circles. Before UV, all samples exhibit Newtonian behavior, i.e., a constant, low viscosity. After UV, all samples display a yield-stress, which is the shear-stress at which the viscosity rapidly plummets from a near-infinite value. In (c), the Sr-EGTA concentration is varied while the alginate is held constant at 2.5 wt % and the PAG-CD at 30 mM. In (d), the PAG-CD concentration is varied while the alginate is again at 2.5 wt % and the Sr-EGTA is at 40 mM.

milled channel substrate and the cover piece. The microchannels were fabricated by mechanical milling using an end mill on a CNC milling machine. Holes for the needle interface were drilled into the substrate plate using a 650 μm drill bit. The machined PMMA plate was sequentially cleaned by DI water and isopropyl alcohol to remove the milling debris, followed by a 24 h degassing step in a 40 °C vacuum oven to remove the residual solvents. After vacuum drying, both the processed PMMA and a raw PMMA chip were oxidized by 8 min of exposure to UV light in the presence of ozone. The oxidized PMMA wafers were immediately mated together and thermally bonded at 85 °C in a hot press under a pressure of 3.45 MPa for 15 min. The world-to-chip interfaces were established by inserting hypodermic stainless steel needles into the 650 μm mating holes, with an additional 30 min of annealing at 85 °C to release the residual stresses from the fitting process. The needle ports on the PMMA chip were connected to syringes with Teflon tubing (I.D. 650 μm). Two different chips were prepared to test different aspects pertaining to the PR fluids. The chip for fluidic valve studies had several channels, each with a rectangular cross section (200 μm height and 300 μm width). The chip for site-specific deposition studies had a single channel with a rectangular cross section (200 μm height and 350 μm width) and this also had three wells (600 μm depth and 500 μm length) separated by 500 μm. Precision syringe pumps (PHD 2000, Harvard Apparatus) were used to control the infusion of fluids into the chip. Optical detection was done by a fluorescence microscope (Olympus MVX10 Macroview) at 2× magnification.

RESULTS AND DISCUSSION

The PR fluids described here have three major components: linear alginate chains as a matrix for a 3-D network, Sr-EGTA as a source of divalent ions (Sr^{2+}) that can cross-link the alginate chains, and the PAG-CD complex as a phototrigger. The role of each component in our scheme is shown in Figure 2. Alginate is a copolymer of α-L-guluronate (G) and β-D-mannuronate (M) units.[41,42] The G-blocks on two chains provide chelating sites to divalent cations, resulting in "egg-box" junctions between the chains.[42,54,55] The higher the ratio of G to M units, the more the cross-links and the stronger the gel. In this study, the alginate used has a relatively high G content (~51%),[28] which facilitates the development of a strong gel.

As a source of divalent cations, we used the Sr-EGTA chelate. Sr-EGTA is highly soluble in water and gives a clear solution when mixed with alginate. Previously, nanoparticles of $CaCO_3$ have been used as a source of divalent cations for alginate

DOI: 10.1021/acsami.6b03826
ACS Appl. Mater. Interfaces 2016, 8, 17529−17538

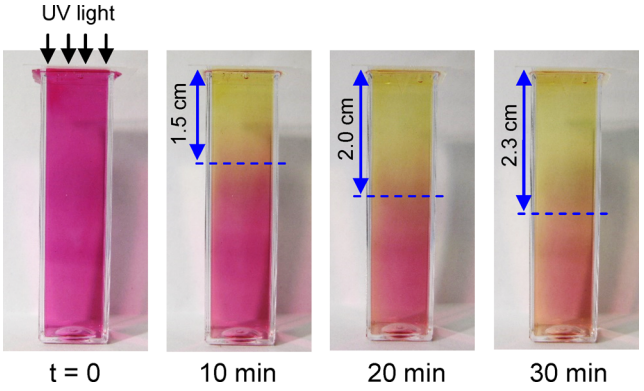

Figure 4. Rate of UV-induced gelation. A quiescent sample of 2.5 wt % alginate, 40 mM Sr-EGTA, 60 mM PAG-CD, and 0.05 mM phenol red is placed in the cuvette and exposed to UV from the top. As the sample gels, its color changes from pink to yellow due to the phenol red. The photos show the gel growing from top to bottom with increasing time. The height of the gel region is marked on each photo.

gelation;[26] however, the particles make the sample turbid and inhomogeneous. If light is used as the trigger for gelation, its penetration depth into such a sample will be low (due to light scattering from the $CaCO_3$ particles). Also, compared to Ca^{2+} ions, Sr^{2+} ions bind stronger to alginate chains, resulting in a stronger gel.[56,57] Consequently, using soluble Sr-EGTA instead of suspended $CaCO_3$ particles is better for PR fluids since it leads to a faster response as well as stronger PR effects. EGTA is a widely used chelating agent.[58] The chelating capacity of EGTA for divalent cations is highly pH-sensitive because of the protonation capability of its moieties (four acetate groups and two nitrogen atoms) at the chelating site. Indeed, the chelating efficiency of EGTA toward Sr^{2+} ions drops sharply around a pH of 7.5, which implies a surge of free Sr^{2+} just below this pH, as shown in the Supporting Information (SI), Figure S1.[59,60] Note that this plot of %released Sr^{2+} vs pH has an inverse sigmoidal shape, indicating a cooperative process. This implies a switch-like response, i.e., a small drop in pH around the threshold pH of 7.5 causes a rapid and appreciable release of free Sr^{2+} into the solution.

We then combined Sr-EGTA (40 mM) with alginate (2.5 wt %) and studied gelation of this mixture in response to pH without using light (Figure S2, SI). As an acid source, D-glucono-δ-lactone (GdL) was added. When GdL is dissolved in water, it is gradually hydrolyzed and decreases the pH of the solution.[61,62] To visualize the pH change, 0.05 mM of phenol red was added. Solutions at various GdL concentrations are all initially nonviscous and exhibit a dark pink color. Thereafter, the color and viscosity change depending on the concentration of GdL. The photos in Figure S2 were acquired 5 h after adding GdL, which is enough time for the complete hydrolysis of GdL. Sample vials are shown inverted to visually indicate the sol to gel transition.[63] The sample at pH 8.0 (10 mM GdL) is pink in color and is a low-viscosity sol. On the other hand, when the sample pH drops below 7.0 (60 and 80 mM GdL), the color turns yellow (due to the colorimetric response of phenol red) and the samples hold their weight in the inverted vials, indicating that they are gels. Thus, the sol–gel transition occurs around a pH 7.5, which is to be expected since this is the threshold pH in Figure S1, below which free Sr^{2+} ions are

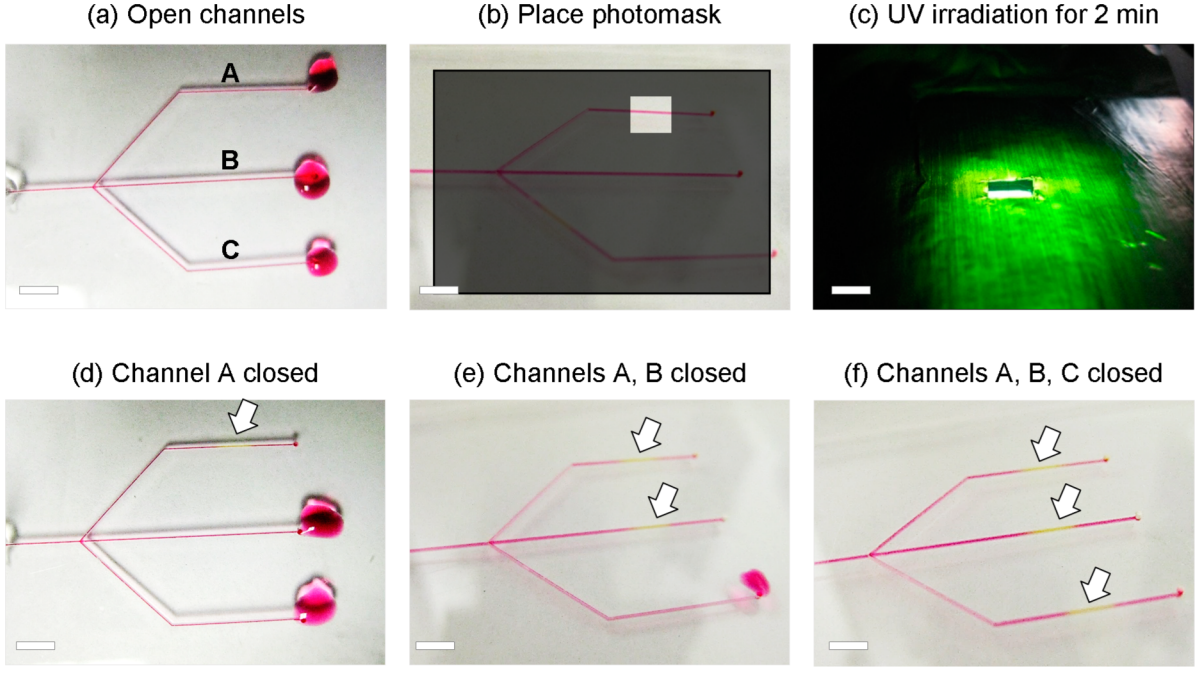

Figure 5. Demonstration of localized flow-blocking using PR fluids. The setup has a main microchannel that branches into three side channels marked A, B, and C. The fluid used here is composed of 2.5 wt % alginate, 40 mM Sr-EGTA, 60 mM PAG-CD, and 0.5 mM phenol red. (a) Initially, all three channels are open and the fluid flows freely out of each. (b) The flow is stopped and a photomask is placed over the setup. (c) A specific portion of channel A (3 mm length) is exposed to UV light for 2 min. (d) When the flow is restarted, it is clear that flow through channel A is blocked. Note that a yellow gel (indicated by arrow) is formed in channel A over the region exposed to UV light. Also, note that channels B and C are still open, i.e., the flow-blocking is done locally and selectively. (e) Next, the same procedure is repeated with channel B, and as a result, flow through channel B is also blocked (but not through channel C). (f) Finally, the procedure is repeated with channel C, and thereby this channel is also blocked. Scale bars in all images correspond to 3 mm. Movie 1 also shows the overall process.

DOI: 10.1021/acsami.6b03826
ACS Appl. Mater. Interfaces 2016, 8, 17529–17538

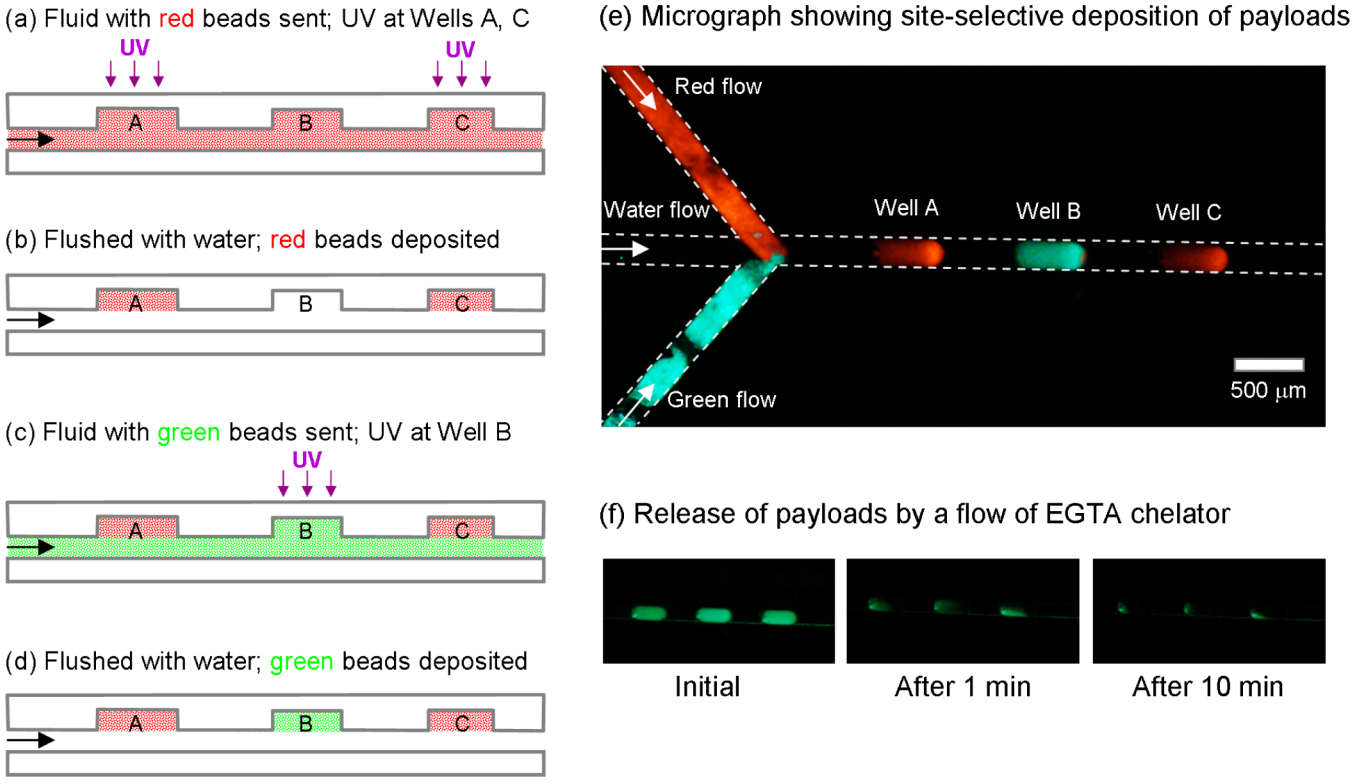

Figure 6. Deposition of payloads at specific addresses within a microchannel. Two PR fluids (composition: 2.5 wt % alginate, 40 mM Sr-EGTA, 60 mM PAG-CD) are prepared with red- and green-fluorescent beads as model payloads. The microchannel is engineered with three wells, marked A, B, and C. (a) First, the fluid with red beads is passed through the channel, and UV light is irradiated for 2 min at the locations of wells A and C. (b) The channel is then flushed with water. At this stage, a gel with red beads is deposited in wells A and C. (c) Next, the fluid with green beads is passed through the channel and UV light is irradiated for 2 min at well B. (d) The channel is again flushed with water, whereupon green beads are localized in a gel in well B. (e) The fluorescence micrograph confirms the site-selective deposition of red and green beads at their respective addresses. (f) Deposited green beads are shown to be released by a flow of EGTA solution through the channel. The decrease in green fluorescence reflects the dissolution of the gel in the wells due to the chelation of Sr^{2+} ions by the EGTA.

released from the Sr-EGTA chelate. Figure S2 shows that the color change of phenol red can be used to visualize the sol−gel transition, and we will employ this property later.

The final element in our PR formulation is a PAG that can be triggered by light. As illustrated in Figure 2c, PAGs typically dissociate under UV light to release H^+ ions, with hydrophobic byproducts also being formed.[49,50] The byproducts are often insoluble, which makes the sample turbid. This turbidity is a problem for our current purpose since it hinders the penetration of light into the sample, thus slowing down the gelation. To solve this problem, we incorporated a cyclodextrin (CD) into our sample. CDs are molecules with hydrophobic cavities that can sequester hydrophobic species,[64,65] such as the byproducts of PAG dissociation. While many types of CDs are available, we chose a methylated β-CD (m-β-CD) due to its high water solubility (>300 mM at 25 °C).[65] The structure of this molecule is shown in Figure S3, and this figure also conceptualizes how the CD captures hydrophobic moieties. Various molar ratios of m-β-CD to the PAG used here (diphenyliodonium nitrate) were examined, and the samples with a molar ratio ≥3 remained transparent during the entire duration of UV exposure. The transparency indicated that there was sufficient m-β-CD to completely sequester the hydrophobic byproducts of PAG photolysis. For this reason, we chose a m-β-CD to PAG molar ratio of 3 for our studies. Thus, in the experiments below, x mM of PAG-CD complex refers to a mixture of x mM of PAG with 3 times that concentration of m-β-CD.

We now proceed to study the response to UV light of our PR fluids. The typical fluid contains 2.5 wt % alginate, 40 mM Sr-EGTA, and 30 mM PAG-CD complex. As shown by Photo A of Figure 3a, this mixture is initially a thin solution that flows freely in the tilted Petri dish. Upon exposure to UV light for 20 min, the solution is converted into a solid gel, and this gel is strong enough that it can be lifted from the Petri dish and held by one's fingers (Photo B). Note that the gel is transparent and homogeneous. Dynamic rheology was then used to quantify gelation. Figure 3 presents plots of the elastic modulus G' and the viscous modulus G'' as a function of the frequency ω for the sample before and after 20 min of UV irradiation. The initial data before UV exposure (Figure 3a) represents a purely viscous response, i.e., G'' is a strong function of ω ($G'' \sim \omega^1$) while G' is negligible and hence not seen on the plot.[34,35] In contrast, after 20 min of UV irradiation (Figure 3b), the sample shows the response of an elastic gel, i.e., $G' > G''$ with both moduli being independent of ω.[34,35] The gel modulus (value of G') is about 2000 Pa, which is among the highest reported in the literature for PR fluids (as noted earlier, all PR fluids are based on self-assembly, i.e., noncovalent bonds). In fact, this modulus is comparable to that of chemically cross-linked alginate bearing methacrylate groups, where covalent bonds are induced between the chains.[43]

DOI: 10.1021/acsami.6b03826
ACS Appl. Mater. Interfaces 2016, 8, 17529−17538

Rheological data were also collected under steady shear. Data for the apparent viscosity η as a function of the shear-stress σ are shown in Figure 3c and d. In Figure 3c, the data are for various Sr-EGTA concentraions combined with 2.5 wt % alginate and 30 mM PAG-CD. Before UV, all samples are Newtonian fluids and have a low viscosity around 0.2 Pa.s. After UV, all samples have a low-shear viscosity that is practically infinite (up to 2 MPa.s) until a critical stress, i.e., the yield stress σ_y is reached. (Once the sample yields, the material tends to get ejected out of the geometry in the rheometer, making the data unreliable;[35] this is why data at high shear stresses are not shown on the plot.) The data confirm that in the gel state, the material has a yield stress, and the magnitude of σ_y increases with Sr-EGTA concentration. For 40 mM Sr-EGTA or higher, σ_y saturates at a value around 100 Pa. Next, data are shown for various concentrations of the PAG-CD complex (Figure 3d), with the alginate fixed at 2.5 wt % and the Sr-EGTA at 40 mM. Here again, the samples show a similar behavior: all are Newtonian fluids before UV and gels with a yield-stress after UV. The yield stress increases with the PAG-CD concentration. At 60 mM of PAG-CD, σ_y is 400 Pa. PAG-CD concentrations above 60 mM were not studied because the sample became translucent due to the solubility limit of the PAG-CD being reached. Note that the higher the PAG-CD, the greater the pH drop upon UV irradiation, and in turn the greater the Sr^{2+} release. Before UV, all samples had a pH of 8.0. After 20 min of UV, the pH dropped to 7.0 for 15 mM PAG-CD and to 6.5 for 60 mM PAG-CD.

It is worth emphasizing that the rheological profile of our PR fluid satisfies the requirements for flow-blocking applications that were noted earlier under Figure 1b. First of all, in the initial state, the fluid behaves as a slightly viscous (Newtonian) liquid, with a viscosity that is independent of shear rate. This means that it can be easily flowed through narrow channels. Conversely, when the fluid is exposed to UV, it is converted to a gel with a yield stress. A simplified model for materials with a yield stress is as a "Bingham plastic".[34,35] This model has been used previously for ER and MR fluids.[4,36] It assumes that there is no flow below the yield stress σ_y and Newtonian flow (constant viscosity) at shear stresses above σ_y. This model is applicable to the present PR fluids, i.e., they can be considered to be switchable between an initial Newtonian liquid before UV to a Bingham plastic after UV. In the Bingham plastic state, flow will be blocked as long as the pressure due to the flow is low (below σ_y). Note that we can increase σ_y further for our fluids by increasing the concentration of alginate (e.g., to 5 or 10 wt %). However, this would increase the viscosity of the initial fluid (and also make it shear-thinning), which would hamper its flowability through microdevices.

Next, we studied the time-dependence of UV-induced gelation. For this, we placed the sample containing 2.5 wt % alginate, 40 mM Sr-EGTA, and 60 mM PAG-CD in a rectangular cuvette (1 cm × 1 cm × 4.5 cm) and covered the top with a glass coverslip. To visualize the pH change and sol−gel transition, the sample also contained 0.05 mM phenol red. UV light was then introduced from the top. As shown in Figure 4, the sample rapidly transforms into a gel starting from the top of the cuvette. Because of the phenol red, the gel layer of the sample has a yellow color while the sol layer is pink (as shown previously in Figure S2). The boundary between the gel and sol layers shifts downward with increasing irradiation time. We estimate the thickness of the gel layer to be 1.5 cm after 10 min and 2.3 cm after 30 min. Gel growth slows down with time: 1.5 cm in the first 10 min, an additional 0.5 cm between 10 and 20 min, and a further 0.3 cm between 20 and 30 min. The reason for this is that the UV light is being directed from the top and its intensity is attenuated as the path length increases. It is important to note that the above response is relatively fast compared to previous PR fluids. Also, PR fluids are typically stirred while being irradiated, which speeds up the response; here, quick gelation is achieved even with the sample in a quiescent state. Overall, it is noteworthy that the current fluid can be converted within 10 min by UV light into a strong gel more than 1 cm thick (i.e., a volume >1 mL).

Having created PR fluids that quickly transform into strong gels, we proceed to test their flow-blocking ability in microchannels. The fluid we used is composed of 2.5 wt % alginate, 40 mM Sr-EGTA, 60 mM PAG-CD, and with 0.5 mM phenol red added for colorimetric observations. This fluid was sent at a flow rate of 5 μL/min through a microchannel that branches into three side channels (Figure 5). Each channel has a rectangular cross section of 200 μm height and 300 μm width. Initially, all channels are open, and the fluid flows out of the three outlets at the end of each branch (Figure 5a). Next, we stopped the flow and placed a photomask to expose a specific region (3 mm long) of Channel A to UV light (Figure 5b,c). After 2 min of UV irradiation, the flow was started again. As shown by Figure 5d, flow through Channel A is now blocked due to the formation of a stong alginate gel in the exposed region. The gel again has a yellow color, as seen earlier in Figures 4 and S2. Note that Channels B and C are still open at this stage. We then repeat the above procedure with Channel B and show that this can be selectively blocked as well (Figure 5e). Lastly, we repeat the same for Channel C (Figure 5f). A movie showing selective closure of a channel is also provided as part of the SI (Movie 1). Note that the channel remains closed for at least 2 h after the light is removed. However, this closure is not permanent. As time progresses, the gel is gradually dissolved by the flow, causing the channel to eventually reopen. We have thus demonstrated a fluidic valve that can be closed by shining light and reopened when the light is removed.

We now briefly discuss the mechanism behind flow-blocking. To a first approximation, flow-blocking requires the gel to be strong enough to withstand the pressure exerted by the flow, i.e., the yield stress of the gel must exceed the pressure drop. Another factor that plays a role is the length of the gelled region in the channel. In our experiments, we found that the gelled region had to be at least 3 mm long. Shorter lengths (1 or 2 mm) of gel failed to stop the flow: in this case, the gel that formed was pushed through as a plug by the flow. This observation suggests that the adhesion of the gel to the inner walls of the channel could be an important factor in blocking the flow. Such adhesion is difficult to quantify because it depends both on the surface energy of the solid substrate (i.e., the wetting of the gel onto the walls) as well as on the surface roughness of the walls (i.e., possible pinning of the gel due to microasperities). It should be noted that our microchannels are made from PMMA, and the native PMMA represents a low-energy surface. To increase the adhesion of the gel to the walls, one could modify the PMMA either chemically (i.e., by introducing functional groups that could form bonds with the alginate) or physically (i.e., by engineering surface roughness). Also, regarding the irradiation time of 2 min to stop the flow, note that this time can be reduced further if the channel walls are made of a UV-transparent material like quartz instead of PMMA, which partially attenuates the incident UV light.

DOI: 10.1021/acsami.6b03826
ACS Appl. Mater. Interfaces 2016, 8, 17529−17538

Next, we demonstrate a different microscale application of our PR fluid, which is for site-selective deposition and release of materials.[66,67] For this application, we used the same fluid composition as above, and we prepared two batches of the fluid with red- and green-fluorescent microbeads, respectively. The microbeads are a model for a payload to be deposited at specific sites. The setup is shown in Figure 6. We used a flow channel with a rectangular cross section (200 μm height and 350 μm width) and three separate wells (600 μm depth and 500 μm length). First, the PR fluid with red beads was sent through the channel. Then, we stopped the flow and used a photomask to expose just wells A and C to UV light for 2 min. This caused an alginate gel with red beads to be deposited in wells A and C. The channel was then flushed with water. Next, the PR fluid with green beads was sent through the channel. The flow was again stopped and well B was exposed to UV for 2 min, followed again by a flush with water. This resulted in an alginate gel with green beads to be deposited in well B. Finally, the deposited alginate gels were reinforced by flowing 30 mM $SrCl_2$ solution. As shown by the fluorescence micrograph in Figure 6e, the model materials (red- and green-fluorescent beads) are selectively deposited in the specific wells. In addition, as shown in Figure 6f, beads deposited in the wells can be released subsequently by flowing EGTA solution through the channel, since EGTA chelates and removes the Sr^{2+} cross-links.

The above concept can be easily extended to other more relevant payloads. Alginate gels are highly biocompatible and have been used to encapsulate proteins, enzymes, cells, and even small organisms like the nematode *C. elegans*.[41,42] Thus, by incorporating such payloads into our PR fluid instead of fluorescent beads, followed by selective deposition of the alginate gel with the pertinent payload, we can potentially fabricate sensors or microreactors with distinct, localized functions.[66,67] Note that the fluid starts at a pH of 8.0 and the final gel has a pH around 6.5. So, the pH range over the operation of the fluid is mostly within a range that is compatible with biological materials. Note also that once the gels are deposited at selected points along a channel, the flow of the alginate fluid can be stopped and one can switch to a different fluid (e.g., bearing nutrients for cell growth).

CONCLUSIONS

In this study, we have described a new biopolymer-based PR fluid. This system addresses several limitations of existing PR fluids that have hampered their applicability. Inexpensive, commercially available chemicals are used to make these fluids, including alginate, Sr-EGTA, PAG, and m-β-CD. The working principle is that upon exposure to UV light, the PAG is photolyzed, which drops the pH and releases Sr^{2+} from its chelate. The latter cross-link alginate chains to form a strong gel (σ_y > 100 Pa). Because the m-β-CD solubilizes the hydrophobic byproducts formed by PAG photolysis, the sample remains transparent before and after UV exposure. Our fluids exhibit a high contrast in rheological properties between their initial and final states (low-viscosity solution before UV and a high-yield-stress-gel after UV). The fluids also show a relatively fast response to UV (1-cm-thick gel formed within 10 min of UV expsosure).

We then demonstrate the use of these fluids in two microfluidic applications. First, we create a light-activated fluidic valve. When a specific point of a microchannel network is exposed to UV light through a mask, the fluid at that point is converted into a strong gel in a few minutes, and the resulting gel blocks the flow through that channel. When the UV light is switched off, the gel undergoes self-dissolution and the channel reopens. In addition, we also demonstrate the site-selective deposition and release of model materials within a microchannel. Both these applications leverage the key advantage of light over other stimuli, which is its ability to be directed at a precise location from a distance.

ASSOCIATED CONTENT

Supporting Information

The Supporting Information is available free of charge on the ACS Publications website at DOI: 10.1021/acsami.6b03826.

Structure of the Sr-EGTA chelate and pH-dependent release of free cations from the chelate (Figure S1); pH-sensitive gelation of alginate combined with Sr-EGTA (Figure S2); structure of the m-β-CD and depiction of how it captures hydrophobic byproducts (Figure S3) (PDF)

Movie demonstrating the light-induced flow-blocking process (AVI)

AUTHOR INFORMATION

Corresponding Author

*E-mail: sraghava@umd.edu.

Notes

The authors declare no competing financial interest.

ACKNOWLEDGMENTS

This work was funded in part by a grant from NSF (CBET-1034215). A.X.L. was supported by a SMART scholarship from the Department of Defense.

REFERENCES

(1) Liu, Y. D.; Choi, H. J. Electrorheological Fluids: Smart Soft Matter and Characteristicsl. *Soft Matter* **2012**, *8*, 11961−11978.

(2) Sheng, P.; Wen, W. J. Electrorheological Fluids: Mechanisms, Dynamics, and Microfluidics Applications. *Annu. Rev. Fluid Mech.* **2012**, *44*, 143−174.

(3) de Vicente, J.; Klingenberg, D. J.; Hidalgo-Alvarez, R. Magnetorheological Fluids: A Review. *Soft Matter* **2011**, *7*, 3701−3710.

(4) Wang, D. H.; Liao, W. H. Magnetorheological Fluid Dampers: A Review of Parametric Modelling. *Smart Mater. Struct.* **2011**, *20*, 023001.

(5) Niu, X. Z.; Wen, W. J.; Lee, Y. K. Electrorheological-Fluid-Based Microvalves. *Appl. Phys. Lett.* **2005**, *87*, 243501.

(6) Wolff, T.; Emming, C. S.; Suck, T. A.; Von Bunau, G. Photorheological Effects in Micellar Solutions Containing Anthracene-Derivatives - A Rheological and Static Low-Angle Light-Scattering Study. *J. Phys. Chem.* **1989**, *93*, 4894−4898.

(7) Sershen, S. R.; Mensing, G. A.; Ng, M.; Halas, N. J.; Beebe, D. J.; West, J. L. Independent Optical Control of Microfluidic Valves Formed from Optomechanically Responsive Nanocomposite Hydrogels. *Adv. Mater.* **2005**, *17*, 1366−1370.

(8) Lee, C. T.; Smith, K. A.; Hatton, T. A. Photoreversible Viscosity Changes and Gelation in Mixtures of Hydrophobically Modified Polyelectrolytes and Photosensitive Surfactants. *Macromolecules* **2004**, *37*, 5397−5405.

(9) Sakai, H.; Orihara, Y.; Kodashima, H.; Matsumura, A.; Ohkubo, T.; Tsuchiya, K.; Abe, M. Photoinduced Reversible Change of Fluid Viscosity. *J. Am. Chem. Soc.* **2005**, *127*, 13454−13455.

(10) Eastoe, J.; Vesperinas, A. Self-assembly of Light-Sensitive Sufactants. *Soft Matter* **2005**, *1*, 338−347.

(11) Chu, Z. L.; Dreiss, C. A.; Feng, Y. J. Smart Wormlike Micelles. *Chem. Soc. Rev.* **2013**, *42*, 7174−7203.

(12) Peng, S. H.; Guo, Q. P.; Hughes, T. C.; Hartley, P. G. Reversible Photorheological Lyotropic Liquid Crystals. *Langmuir* **2014**, *30*, 866−872.
(13) Lin, Y. Y.; Cheng, X. H.; Qiao, Y.; Yu, C. L.; Li, Z. B.; Yan, Y.; Huang, J. B. Creation of Photo-Modulated Multi-State and Multi-Scale Molecular Assemblies via Binary-State Molecular Switch. *Soft Matter* **2010**, *6*, 902−908.
(14) Lu, Y. C.; Zhou, T. F.; Fan, Q.; Dong, J. F.; Li, X. F. Light-Responsive Viscoelastic Fluids Based on Anionic Wormlike Micelles. *J. Colloid Interface Sci.* **2013**, *412*, 107−111.
(15) Zhang, J. Q.; Jin, J. Y.; Zou, L.; Tian, H. Reversible Photo-Controllable Gels Based on Bisthienylethene-Doped Lecithin Micelles. *Chem. Commun.* **2013**, *49*, 9926−9928.
(16) Tomatsu, I.; Hashidzume, A.; Harada, A. Contrast Viscosity Changes Upon Photoirradiation for Mixtures of Poly(Acrylic Acid)-Based Alpha-Cyclodextrin and Azobenzene Polymers. *J. Am. Chem. Soc.* **2006**, *128*, 2226−2227.
(17) Deshmukh, S.; Bromberg, L.; Smith, K. A.; Hatton, T. A. Photoresponsive Behavior of Amphiphilic Copolymers of Azobenzene and N,N-Dimethylacrylamide in Aqueous Solutions. *Langmuir* **2009**, *25*, 3459−3466.
(18) Chen, D.; Liu, H.; Kobayashi, T.; Yu, H. F. Multiresponsive Reversible Gels Based on a Carboxylic Azo Polymer. *J. Mater. Chem.* **2010**, *20*, 3610−3614.
(19) Paulusse, J. M. J.; Sijbesma, R. P. Molecule-Based Rheology Switching. *Angew. Chem., Int. Ed.* **2006**, *45*, 2334−2337.
(20) Matsumoto, S.; Yamaguchi, S.; Ueno, S.; Komatsu, H.; Ikeda, M.; Ishizuka, K.; Iko, Y.; Tabata, K. V.; Aoki, H.; Ito, S.; Noji, H.; Hamachi, I. Photo Gel-Sol/Sol-Gel Transition and its Patterning of a Supramolecular Hydrogel as Stimuli-Responsive Biomaterials. *Chem. - Eur. J.* **2008**, *14*, 3977−3986.
(21) Rajaganesh, R.; Gopal, A.; Mohan Das, T.; Ajayaghosh, A. Synthesis and Properties of Amphiphilic Photoresponsive Gelators for Aromatic Solvents. *Org. Lett.* **2012**, *14*, 748−751.
(22) Ketner, A. M.; Kumar, R.; Davies, T. S.; Elder, P. W.; Raghavan, S. R. A Simple Class of Photorheological Fluids: Surfactant Solutions with Viscosity Tunable by Light. *J. Am. Chem. Soc.* **2007**, *129*, 1553−1559.
(23) Kumar, R.; Raghavan, S. R. Photogelling Fluids Based on Light-Activated Growth of Zwitterionic Wormlike Micelles. *Soft Matter* **2009**, *5*, 797−803.
(24) Sun, K. S.; Kumar, R.; Falvey, D. E.; Raghavan, S. R. Photogelling Colloidal Dispersions Based on Light-Activated Assembly of Nanoparticles. *J. Am. Chem. Soc.* **2009**, *131*, 7135−7141.
(25) Kumar, R.; Ketner, A. M.; Raghavan, S. R. Nonaqueous Photorheological Fluids Based on Light-Responsive Reverse Wormlike Micelles. *Langmuir* **2010**, *26*, 5405−5411.
(26) Javvaji, V.; Baradwaj, A. G.; Payne, G. F.; Raghavan, S. R. Light-Activated Ionic Gelation of Common Biopolymers. *Langmuir* **2011**, *27*, 12591−12596.
(27) Lee, H. Y.; Diehn, K. K.; Sun, K. S.; Chen, T. H.; Raghavan, S. R. Reversible Photorheological Fluids Based on Spiropyran-Doped Reverse Micelles. *J. Am. Chem. Soc.* **2011**, *133*, 8461−8463.
(28) Oh, H.; Javvaji, V.; Yaraghi, N. A.; Abezgauz, L.; Danino, D.; Raghavan, S. R. Light-Induced Transformation of Vesicles to Micelles and Vesicle-Gels to Sols. *Soft Matter* **2013**, *9*, 11576−11584.
(29) Oh, H.; Ketner, A. M.; Heymann, R.; Kesselman, E.; Danino, D.; Falvey, D. E.; Raghavan, S. R. A Simple Route to Fluids with Photo-Switchable Viscosities Based on a Reversible Transition Between Vesicles and Wormlike Micelles. *Soft Matter* **2013**, *9*, 5025−5033.
(30) Baglioni, P.; Braccalenti, E.; Carretti, E.; Germani, R.; Goracci, L.; Savelli, G.; Tiecco, M. Surfactant-Based Photorheological Fluids: Effect of the Surfactant Structure. *Langmuir* **2009**, *25*, 5467−5475.
(31) Juggernauth, K. A.; Gros, A. E.; Meznarich, N. A. K.; Love, B. J. In situ Photogelation Kinetics of Laponite Nanoparticle-Based Photorheological Dispersions. *Soft Matter* **2011**, *7*, 10108−10115.
(32) Matsumura, A.; Sakai, K.; Sakai, H.; Abe, M. Photoinduced Increase in Surfactant Solution Viscosity Using Azobenzene Dicarboxylate for Molecular Switching. *J. Oleo Sci.* **2011**, *60*, 203−207.
(33) Stone, H. A.; Stroock, A. D.; Ajdari, A. Engineering Flows in Small Devices: Microfluidics Toward a Lab-on-a-chip. *Annu. Rev. Fluid Mech.* **2004**, *36*, 381−411.
(34) Squires, T. M.; Quake, S. R. Microfluidics: Fluid Physics at the Nanoliter Scale. *Rev. Mod. Phys.* **2005**, *77*, 977−1026.
(35) Macosko, C. W. *Rheology: Principles, Measurements, and Applications*; Wiley-VCH: New York, 1994.
(36) Larson, R. G. *The Structure and Rheology of Complex Fluids*; Oxford University Press: New York, 1999.
(37) Dimock, G. A.; Yoo, J. H.; Wereley, N. M. Quasi-Steady Bingham Biplastic Analysis of Electrorheological and Magneto-rheological Dampers. *J. Intell. Mater. Syst. Struct.* **2002**, *13*, 549−559.
(38) Piepenbrock, M. O. M.; Lloyd, G. O.; Clarke, N.; Steed, J. W. Metal- and Anion-Binding Supramolecular Gels. *Chem. Rev.* **2010**, *110*, 1960−2004.
(39) Babu, S. S.; Praveen, V. K.; Ajayaghosh, A. Functional pi-Gelators and Their Applications. *Chem. Rev.* **2014**, *114*, 1973−2129.
(40) Weiss, R. G. The Past, Present, and Future of Molecular Gels. What is the Status of the Field, and Where is it Going? *J. Am. Chem. Soc.* **2014**, *136*, 7519−7530.
(41) Augst, A. D.; Kong, H. J.; Mooney, D. J. Alginate Hydrogels as Biomaterials. *Macromol. Biosci.* **2006**, *6*, 623−633.
(42) Lee, K. Y.; Mooney, D. J. Alginate: Properties and Biomedical Applications. *Prog. Polym. Sci.* **2012**, *37*, 106−126.
(43) Jeon, O.; Bouhadir, K. H.; Mansour, J. M.; Alsberg, E. Photocrosslinked Alginate Hydrogels with Tunable Biodegradation Rates and Mechanical Properties. *Biomaterials* **2009**, *30*, 2724−2734.
(44) Bonino, C. A.; Samorezov, J. E.; Jeon, O.; Alsberg, E.; Khan, S. A. Real-Time *in situ* Rheology of Alginate Hydrogel Photocrosslinking. *Soft Matter* **2011**, *7*, 11510−11517.
(45) Chueh, B. H.; Zheng, Y.; Torisawa, Y. S.; Hsiao, A. Y.; Ge, C. X.; Hsiong, S.; Huebsch, N.; Franceschi, R.; Mooney, D. J.; Takayama, S. Patterning Alginate Hydrogels Using Light-Directed Release of Caged Calcium in a Microfluidic Device. *Biomed. Microdevices* **2010**, *12*, 145−151.
(46) Cui, J. X.; Wang, M.; Zheng, Y. J.; Rodriguez Muniz, G. M.; del Campo, A. Light-Triggered Cross-Linking of Alginates with Caged Ca2+. *Biomacromolecules* **2013**, *14*, 1251−1256.
(47) Higham, A. K.; Bonino, C. A.; Raghavan, S. R.; Khan, S. A. Photo-activated Ionic Gelation of Alginate Hydrogel: Real-Time Rheological Monitoring of the Two-Step Crosslinking Mechanism. *Soft Matter* **2014**, *10*, 4990−5002.
(48) Stowers, R. S.; Allen, S. C.; Suggs, L. J. Dynamic Phototuning of 3D Hydrogel Stiffness. *Proc. Natl. Acad. Sci. U. S. A.* **2015**, *112*, 1953−1958.
(49) Dektar, J. L.; Hacker, N. P. Photochemistry of Diaryliodonium Salts. *J. Org. Chem.* **1990**, *55*, 639−647.
(50) Reichmanis, E.; Houlihan, F. M.; Nalamasu, O.; Neenan, T. X. Chemical Amplification Mechanisms for Microlithography. *Chem. Mater.* **1991**, *3*, 394−407.
(51) Raeburn, J.; McDonald, T. O.; Adams, D. J. Dipeptide Hydrogelation Triggered via Ultraviolet Light. *Chem. Commun.* **2012**, *48*, 9355−9357.
(52) Fameau, A. L.; Arnould, A.; Lehmann, M.; von Klitzing, R. Photoresponsive Self-Assemblies Based on Fatty Acids. *Chem. Commun.* **2015**, *51*, 2907−2910.
(53) Okoye, N. H.; de Silva, U. K.; Wengatz, J. A.; Lapitsky, Y. Photodirected Assembly of Polyelectrolyte Complexes. *Polymer* **2015**, *60*, 69−76.
(54) Sikorski, P.; Mo, F.; Skjak-Braek, G.; Stokke, B. T. Evidence for Egg-Box-Compatible Interactions in Calcium-Alginate Gels from Fiber X-Ray Diffraction. *Biomacromolecules* **2007**, *8*, 2098−2103.
(55) Fang, Y. P.; Al-Assaf, S.; Phillips, G. O.; Nishinari, K.; Funami, T.; Williams, P. A.; Li, L. B. Multiple Steps and Critical Behaviors of the Binding of Calcium to Alginate. *J. Phys. Chem. B* **2007**, *111*, 2456−2462.

DOI: 10.1021/acsami.6b03826
ACS Appl. Mater. Interfaces 2016, 8, 17529−17538

(56) Morch, Y. A.; Donati, I.; Strand, B. L. Effect of Ca2+, Ba2+, and Sr2+ on Alginate Microbeads. *Biomacromolecules* **2006**, *7*, 1471−1480.
(57) Wideroe, H.; Danielsen, S. Evaluation of the Use of Sr2+ in Alginate Immobilization of Cells. *Naturwissenschaften* **2001**, *88*, 224−228.
(58) EllisDavies, G. C. R.; Kaplan, J. H.; Barsotti, R. J. Laser Photolysis of Caged Calcium: Rates of Calcium Release by Nitrophenyl-EGTA and DM-Nitrophen. *Biophys. J.* **1996**, *70*, 1006−1016.
(59) Patton, C.; Thompson, S.; Epel, D. Some Precautions in Using Chelators to Buffer Metals in Biological Solutions. *Cell Calcium* **2004**, *35*, 427−431.
(60) Patton, C. *MaxChelator*; http://maxchelator.stanford.edu/maxc.html, 2014.
(61) Kuo, C. K.; Ma, P. X. Ionically Crosslinked Alginate Hydrogels as Scaffolds for Tissue Engineering: Part 1. Structure, Gelation Rate and Mechanical Properties. *Biomaterials* **2001**, *22*, 511−521.
(62) Poncelet, D.; Babak, V.; Dulieu, C.; Picot, A. A Physico-Chemical Approach to Production Of Alginate Beads by Emulsification-Internal Ionotropic Gelation. *Colloids Surf., A* **1999**, *155*, 171−176.
(63) Raghavan, S. R.; Cipriano, B. H. "Gel Formation: Phase Diagrams Using Tabletop Rheology and Calorimetry. in *Molecular Gels*; Weiss, R. G., Terech, P., Eds.; Springer: Dordrecht, 2005; pp 233−244.
(64) Szejtli, J. Introduction and General Overview of Cyclodextrin Chemistry. *Chem. Rev.* **1998**, *98*, 1743−1753.
(65) Loftsson, T.; Brewster, M. E. Pharmaceutical Applications of Cyclodextrins 0.1. Drug Solubilization and Stabilization. *J. Pharm. Sci.* **1996**, *85*, 1017−1025.
(66) Shi, X. W.; Tsao, C. Y.; Yang, X. H.; Liu, Y.; Dykstra, P.; Rubloff, G. W.; Ghodssi, R.; Bentley, W. E.; Payne, G. F. Electroaddressing of Cell Populations by Co-Deposition with Calcium Alginate Hydrogels. *Adv. Funct. Mater.* **2009**, *19*, 2074−2080.
(67) Zawko, S. A.; Schmidt, C. E. Simple Benchtop Patterning of Hydrogel Grids for Living Cell Microarrays. *Lab Chip* **2010**, *10*, 379−383.

DOI: 10.1021/acsami.6b03826
ACS Appl. Mater. Interfaces 2016, 8, 17529−17538

Supporting Information for:

Light-Directed Self-Assembly of Robust Alginate Gels at Precise Locations in Microfluidic Channels

Hyuntaek Oh,[1] Annie Xi Lu,[1] Vishal Javvaji,[1] Don L. DeVoe[2] and Srinivasa R. Raghavan[1]*
[1]Department of Chemical and Biomolecular Engineering, University of Maryland, College Park, MD 20742-2111
[2]Department of Mechanical Engineering, University of Maryland, College Park, Maryland 20742, USA
*Corresponding author. Email: sraghava@umd.edu

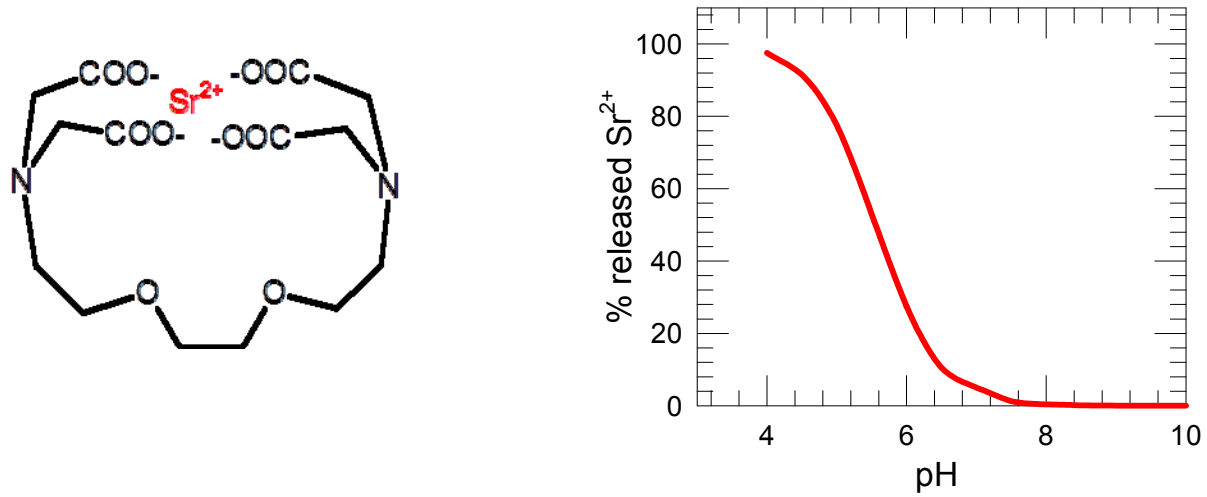

Figure S1. (Left) Chemical structure of the Sr-EGTA chelate. (Right) pH-dependent release of free Sr^{2+} ions from the Sr-EGTA chelate. As pH drops below 7.5, Sr^{2+} ions are increasingly released, with the curve showing an inverse sigmoidal pattern. (Data obtained using MaxChelator: http://maxchelator.stanford.edu/maxc.html)

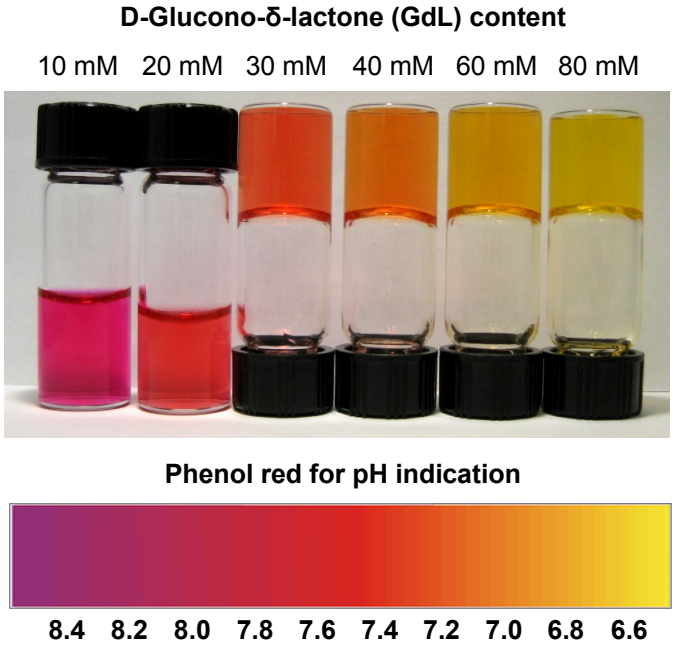

Figure S2. pH sensitive gelation of alginate (2.5 wt%) combined with 40 mM Sr-EGTA. 0.05 mM of phenol red wad added as a pH indicator. To alter the pH, different amounts of GdL were added, as shown above each vial. GdL gradually undergoes hydrolysis and decreases the solution pH. The photos were taken 5 h after GdL addition. When the solution pH drops below 7.5, free Sr^{2+} is released from the chelate, causing gelation of alginate. Gelled samples hold their weight in the inverted vials. As a reference, the color of phenol red at different pH is presented at the bottom.

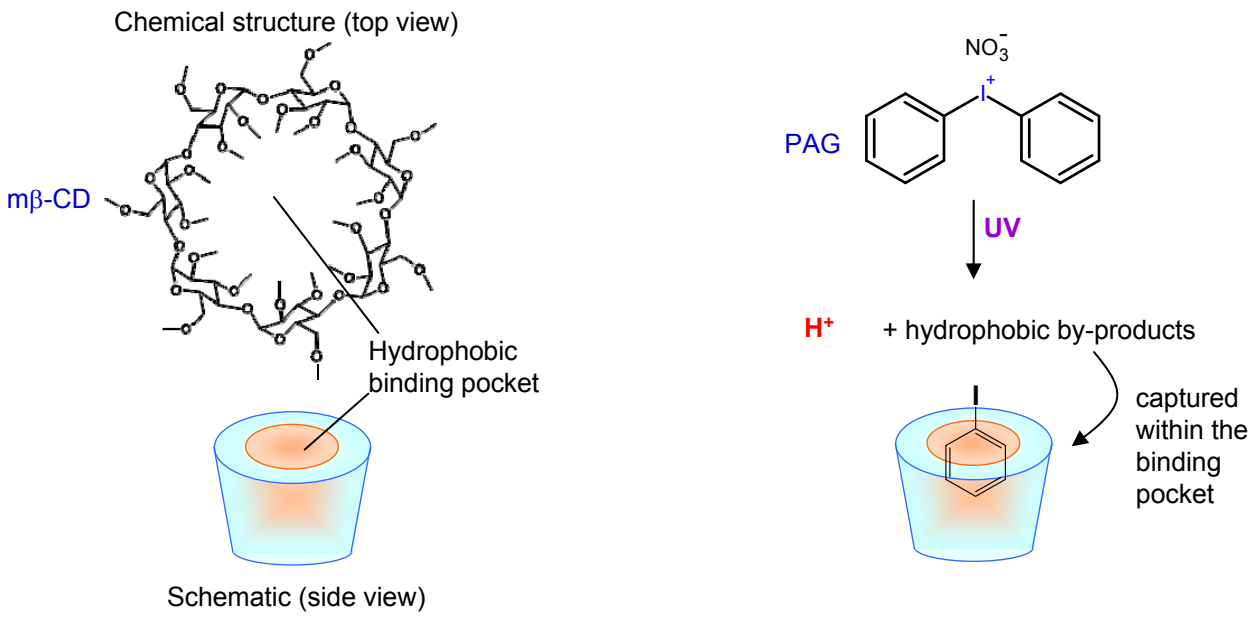

Figure S3. (Left) Chemical structure and schematic of the mβ-CD. The supramolecule has a hydrophilic exterior and a hydrophobic binding pocket in its core. (Right) Photolysis of the PAG (diphenyliodonium nitrate) produces hydrophobic by-products like iodobenzene, which get captured (sequestered) within the binding pocket of the mβ-CD.